Atmospheric and internal turbulence measured on the Very Large Telescope Interferometer with VINCI

Emmanuel Di Folco[1], Bertrand Koehler[1], Pierre Kervella[2], Marc Sarazin[1], Vincent Coudé du Foresto[3], Markus Schöller[2], Markus Wittkowski[2]

[1]European Southern Observatory, K. Schwarzschild Straße 2, D-85748 Garching, Germany
[2]European Southern Observatory - Vitacura, Chile
[3]Observatoire de Paris-Meudon, 5 place J. Janssen, F-92195 Meudon, France

ABSTRACT

In March 2001, the commissioning instrument of the VLTI, VINCI, succeeded in obtaining its first fringes by linking two 40cm aperture siderostats on a 16m baseline. During the first year of operation, thousands of interferometric observations on different baselines were carried out, with the technical goal of characterizing this complex system. We report in this paper these first measurements and estimate the main parameters of the atmospheric and internal turbulence along the complete light path.

We first illustrate the degradation of the visibility accuracy caused by the differential piston and evaluate the contribution of the internal optical path fluctuations with respect to the atmospheric ones. The stability of the VLTI complex is demonstrated, which enabled us to record easily fringes with Unit Telescopes (UTs) on baselines as long as 102.5 m (November 2001). In the last part, infrared measurements of the atmospheric differential piston are reported. They were obtained with the siderostats on two different baselines ranging from 16m to 66m.

Estimations of the coherence time at Cerro Paranal are derived from these commissioning data and compared to the values predicted by the Astronomic Site Monitor (ASM). Finally, constraints on the outer scale length are discussed.

Keywords: Interferometry, atmospheric degradation, turbulence, differential piston, coherence time, outer scale

INTRODUCTION

Astrophysical observations with ground based telescopes are corrupted by the image degradation due to the atmospheric turbulence. Most of the largest monolithic telescopes have now (or will soon) partly overcome this limitation by developing adaptive optics systems in order to compensate for wave-front corrugations and offer sharp images with long exposure times. For mean seeing conditions in good sites, the images obtained are therefore quasi diffraction-limited and their spatial resolution is thus determined by the diameter of the primary mirror. However mirror diameters are physically limited to a few tens of meters and the largest mirrors under consideration do not exceed 50 to 100m.

Ignoring these limitations, long baseline interferometry offers very high spatial resolution capability for astronomical observations, the highest spatial frequency being defined by the ratio between the observing wavelength and the distance between the telescopes. Most of interferometers in operation make use of baselines of a ten to a few hundreds of meters and use visible or near-infrared detection, thus allowing submilliarcsecond measurements or imaging.

However, interferometric techniques at visible or infrared wavelengths do not remain free from atmospheric turbulence damages. By combining the wave-fronts intercepted by two (or more) identical telescopes, interferometric measurements suffer from two main restrictions (spatial and temporal effects). First, the degradation of the images under the influence of the atmospheric turbulence limits the sensitivity of the instrument, i.e. the total amount of flux used for recombination. The second one is the jitter of the interference fringes during the exposure time due to the temporal variations of the differential optical path between the arms of the instrument. This latter effect limits severely both precision (degrading to the contrast of the fringes) and sensitivity (limiting indirectly the acceptable exposure time).

The former is well known and can be corrected by installing adaptive optics systems on each telescope, the second one can be partially compensated for with a servo-loop instrument tracking the fringes. Improving our knowledge of these atmospheric perturbations is thus useful in order first to adapt the observing strategy and then to prepare the future fringe tracking instruments whose bandwidth –and thus performances- will strongly depend on the statistical properties of the atmospheric fluctuations. We present in this paper the first measurements of the differential piston on the VLTI. Differential piston is responsible for the motion and deformation of the fringes during the observation and is the main limit to the precision of the instrument in the high flux regime.

1. INFLUENCE OF THE DIFFERENTIAL PISTON ON VINCI INTERFEROMETRIC DATA

1. The classical seeing theory

In the simple Kolmogorov model of the turbulence, the atmosphere is usually described as a single turbulent layer in which the variations of the refractive index with temperature and pressure induce both phase and amplitude fluctuations on the propagating stellar wave-front. In addition, it is usually assumed that the time scale of temporal changes in the layer is much smaller than the time it takes the wind to blow the turbulence over the telescope aperture (Taylor's hypothesis of frozen turbulence). The spatial and temporal properties of this single layer are linked by the wind speed of the layer. We will focus our study on the perturbations of the phase induced by the fluctuations of the refraction index.

These perturbations can be easily described with the spatial structure function of the phase $D\Phi(r)$, which is defined as the mean squared difference between the phases at two points r and r' of the wave-front at a given time t.

$$D\Phi_t(r,dh) \equiv \left\langle \left[\Phi_t(r') - \Phi_t(r+r')\right]^2 \right\rangle = 2.91 k^2 C_n^2 dh r^{5/3} \quad (^{13})$$

where $k=2\pi/\lambda$ is the spatial frequency, C_n^2 the constant structure of the refraction index, dh the depth of the turbulent layer. The integration over the whole atmosphere (z being the zenithal distance) leads to:

$$D\Phi_r(t) = 6.88\left(\frac{r}{r_0}\right)^{5/3} \text{ with } r_0 \propto \left[\lambda^{-2}\sec(z)\int_0^{\infty} C_n^2(h)dh\right]^{-3/5}$$

The introduced Fried's parameter, r_0, defines the coherence length of the atmosphere and practically limits the spatial resolution of the images obtained with a classical telescope. It corresponds to the diameter of a wave-front patch over which the standard deviation of the phase fluctuations is approximately 1 rad.

Under Taylor's hypothesis of a frozen turbulence, the temporal fluctuations of the phase can be similarly described using the temporal phase structure function $D\Phi(t)$ at any given point r of the perturbed wave-front:

$$D\Phi_r(t) \equiv \left\langle \left[\Phi_r(t') - \Phi_r(t+t')\right]^2 \right\rangle = \left(\frac{t}{t_0}\right)^{5/3}$$

This equation defines the coherence time of the turbulent atmosphere t_0. It corresponds to the duration over which the standard deviation of the phase fluctuations at a given point is of the order of 1 rad. These two scaling parameters r_0 and t_0 describe the strength and the rapidity of the turbulence degrading the images obtained in the classical monopupil imaging mode. They can be linked together by the average velocity of the turbulence (equivalent wind speed V):

$$t_0 = 0.31\frac{r_0}{V} \quad (^{13})$$

2. Seeing theory applied to interferometry

In the case of interferometric observations with two telescopes, the properties of distant areas of the wave-front have to be compared. The atmospheric perturbations introduce in each pupil (separated by the baseline length) a mean delay corresponding to the phase of each wave-front averaged over the surface of the mirrors. This piston term is the zero order of the Zernike polynomials and does not affect the image of a single telescope but introduces in our case a random delay between both arms of the interferometer. This differential phase (or differential piston) between both wave-fronts makes the fringes move across the detector and tends to blur the fringe pattern, thus degrading the contrast to be measured.

This differential delay being assumed to have a Gaussian statistics, its standard deviation depends on the baseline length (B) of the interferometer and on the Fried parameter: $\sigma_{OPD} = \frac{2.62}{2\pi}\lambda_0\left(\frac{B}{r_0}\right)^{5/6}$, which is in the end independent of the wavelength since $r_0 \propto \lambda^{6/5}$. The temporal power spectrum of the differential piston shows in theory three different domains, as described by Conan ([4]) based on an infinite outer scale model (L_0). They are separated by two cutoff frequencies f_1 = 0.2 V/B and f_2 = 0.3 V/D, with V the mean wind speed of the turbulent layer, B the interferometer baseline and D the diameter of the telescopes. The corresponding power slopes are from low to high frequency -2/3, -8/3 and -17/3. Numerous experimental data show evidence of a finite outer scale ranging from a few tens to a few hundreds of meters [5,11,12]. It results in a saturation of the fluctuations of the differential piston and the power spectrum is flat for $f < f_0 \sim V/L_0$ (Von Karman description). When L_0 is greater or of the order of the baseline length, only one break can be seen in the spectrum. The effect of the coherence time on the spectrum is a simple scaling of the -8/3 slope in the intermediate frequency range (cf §3.2).

Another definition of the coherence time [3] is the interferometric coherence time T_0, defined as the time interval during which the variance of the differential phase between both beams -and hence the fringes jitter- does not exceed 1 rad^2. It is linked to the single aperture coherence time t_0 by the relation T_0=2.58 t_0 (t_0 is mainly used in adaptive optics systems). Like r_0 and t_0, the interferometric coherence time depends strongly on the observing wavelength: $T_0 \propto \lambda^{6/5}$. It is typically of the order of 25 ms in the visible (0.5 μm) and hence about 250 ms in the near infrared (2.2 μm). Even if T_0 is more natural to describe the influence of the turbulence on interferometric observations, we will only refer in this paper to the single aperture definition t_0 at λ_0=0.5 μm. This latter is indeed more appropriate for comparisons with previous long term studies on the atmospheric parameters at Paranal.

3. VINCI in the VLTI

All measurements reported in this paper were obtained with the commissioning instrument of the VLTI. VINCI is a technical instrument based on single-mode fluoride glass fibers and coupler that enables coaxial combination of two beams in the K band (2.0 – 2.4 μm) (see [8] for extensive description). Optical fibers filter out the spatial modes of the turbulence and convert into photometric variations the wave-front corrugations caused by the atmosphere (except for the piston). In order to correct interferograms of photometric variations, each incoming beam is split in two parts before the coherent combination.

The inteferogram is produced by a temporal modulation: the optical path is scanned with a piezo-mirror over a few hundreds of microns around the zero optical path difference (zero-OPD). An infrared Hawaii camera is used for the detection in the K band on four pixels (two photometric channels and two phase-opposite interferometric ones). Extension of the spectral capability of VINCI was successfully tested in June 2002 thanks to the IONIC experiment, an integrated optics chip that allows combining the 2 beams in the H band [7].

On sky, two 40cm aperture siderostats were used for routine observations. The beams can cover up to 150 m each (through the delay lines tunnel) on the shortest baseline used (16m). Two delay lines are used in order to compensate for the differential delay between both wave-fronts before recombination. In order to compensate for the geometric delay due to star motion, a trajectory is computed for the tracking delay line (DL) according to the coordinates of the target. Its precision depends on the knowledge of the baseline (i.e. the positions of each siderostat on the ATs stations). The OPD models currently used on the VLTI enable to detect the fringes typically within a few hundreds of microns. This range being small enough to find them after only a short DL scan, the OPD models have not been refined yet to the level required for the most demanding observations modes such as astrometry with PRIMA.

In addition to this geometrical offset, the random fringe packet motion is corrected after each scan. A simple fringe envelop centroid algorithm is applied to each scan and the correction, translated into optical path delay, results in an offset sent to the tracking DL. This basic coherencing capability allows centering the fringes with an accuracy of about one fringe (~2 μm) with good interferometric signal to noise ratio (SNR). It permits thus in theory to keep the fringe packet within a fraction of the coherence length during a batch of several hundreds of scans.

4. Degradation of the visibility and precision of the measurements

The effect of the piston on interferometric data provokes a distortion of the fringes due to the jitter of the zero OPD during the scan, which blurs the fringes pattern. The frequency of the fringes themselves is then modulated inside each scan and the resulting fringe peak in the spectrum can be enlarged and shifted. Since the interferometric observable is the squared visibility (μ^2) –measured by integrating the power of the fringe peak at the fringes frequency- its estimation is degraded by the piston speed which is related to the coherence time of the atmosphere. It is therefore necessary to adapt the scan frequency to the state of the atmosphere during the observations. Since a faster scanning speed will reduce the degradation caused by the piston, but also the global photometric SNR, a compromise has to be found.

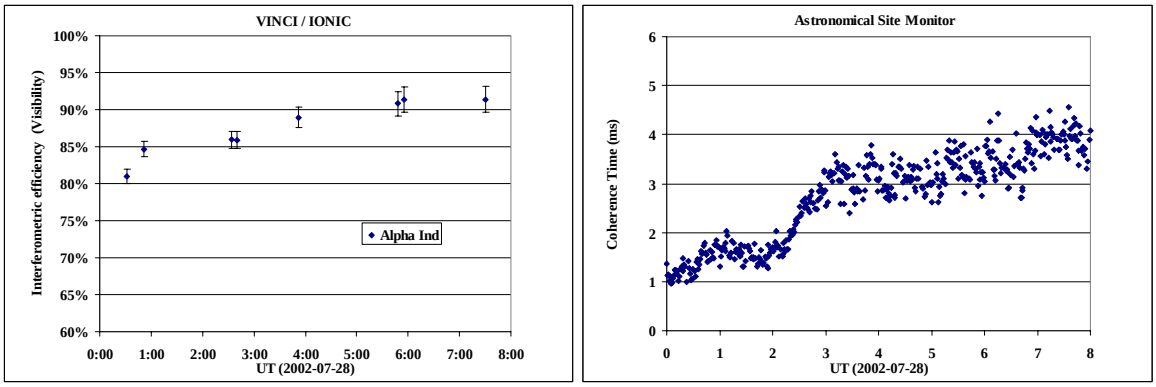

Figure 1. Intra night variations of the raw visibilities due to variations of the atmospheric transfer function at low acquisition frequency with VINCI/IONIC in the H band (Courtesy of P. Kern, LAOG). Correlation with ASM estimations of the coherence time is put in evidence.

Figure 1 illustrates the intra night variations of the atmospheric transfer function. The interferometric efficiency (auto-calibrated visibilities of a single well known calibrator) includes the atmospheric and instrumental effects but the latter have proved to be stable within 1-2 % ([9]). The major cause for the plotted variations is though to be originated from the atmosphere. This points out the fact that calibrator stars used for absolute visibility estimation must be observed at the same frequency(ies) as their related scientific target and if possible with the same t_0 (as close as possible to the scientific target). The correlation between the degradation of the inteferometric efficiency and the coherence time is especially clear when the scanning frequency is low. This was the case with IONIC in the H band. Similar correlations were occasionally observed with MONA but the acquisition frequency being usually faster, the amplitude of the variations is shallower and the resulting function transfer is relatively stable.

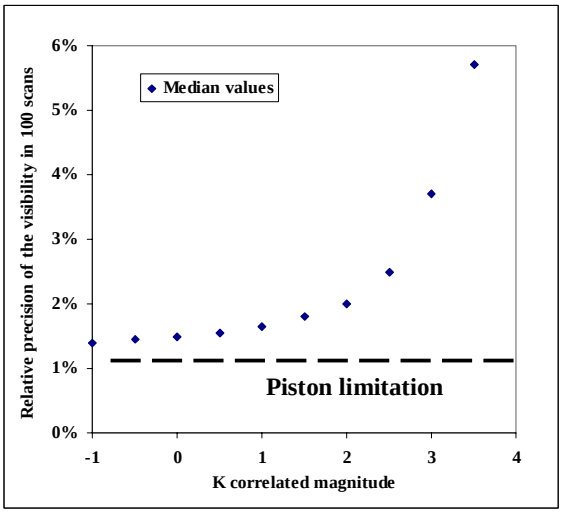

The OPD fluctuations are a severe limit to the visibilities accuracy that only implementation of a fringe tracker can overcome. Figure 2 shows that the piston effect is the main limit to the precision of our visibility measurements on bright stars for which the integration time is the shortest. Current estimations of the squared visibilities through the integration of the power are limited to typically 1-2 % in accuracy with 100 scans. The evolution of the mean relative precision of the visibilities measured with the siderostats is plotted against the correlated magnitude defined by: $m_{cor} = -2.5\ \mathrm{Log}(\mu^2 10^{-m/2.5})$. Future installation of fringe trackers on the VLTI (first FINITO and then FSU/PRIMA) will considerably improve this precision.

Figure 2. Schematic variations of the relative precision of VINCI visibilities against the K correlated magnitude and influence of the piston.

2. INTERNAL STABILITY OF THE VLTI

1. Laboratory measurements with artificial light

1.1. Auto-test in the interferometric laboratory

The artificial light sources available consist of two thermal lamps in an integrating sphere and a K-band Laser with a central wavelength of 2.3 μm. The light is injected with a K band single mode fiber into the optical path and separated with two beam splitter cubes, thus simulating two plane stellar wave-fronts feeding the instrument. In this so called auto-test mode, the light is directed towards the injection stages and the coupler without passing through the delay lines tunnel. It provides then a very stable flux for technical and routine tests since the air flow in the interferometric laboratory has shown to be extremely stable.

1.2. Auto-collimation including the Delay Lines tunnel

Using the more powerful infrared laser, the light can be sent backwards through the complete optical path including the delay lines up to the entrance of the AT stations pits where corner cubes are installed in order to retro-reflect the beams towards the combination instrument. This mode is called auto-collimation and allows probing the internal atmosphere of the interferometric complex. The primary mirrors of the siderostats can also be used as retro-reflectors in place of the corner cubes.

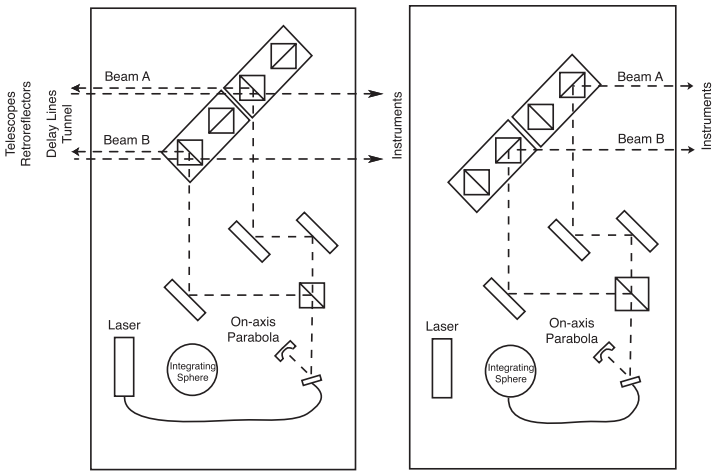

Figure 3. Principle of internal measurements in auto-collimation (left) and auto-test (right)

2. Stability of the interferometric laboratory

The most common algorithm used to estimate the phase of a sinusoidal signal is the so called ABCD algorithm, in which the signal is integrated over four bins corresponding to four points of modulation per fringe. It has been suggested by Cassaing [2] that a fringe tracker which does not aim at providing the visibility in addition to the phase information can work with only two modulation points per fringe. The so called AC algorithm therefore uses only two phase-opposite interferometric outputs in order to derive the phase information. Its dynamic is smaller than the ABCD one since its linear part is shorter than λ/2 but it provides a gain in term of SNR. The demodulated signal is S: $S = \mathrm{A}\sin\left(\frac{1}{V}\frac{A-C}{A+C}\right)$ where V is the contrast of the locked-fringe and A, C the flux in each interferometric output.

We took advantage of the two phase-opposite outputs of VINCI in order to avoid temporal modulation and to obtain information on the phase at very high frequency (typically f ~ 3 kHz) whereas the regular scans recorded are usually limited by the maximum speed of the piezo-mirror. Applying this method obviously requires very high stability of the fringe pattern on the detector so that the pixels are always located on the same fringe. It was therefore used in auto-test mode only in order to verify that the vibrations produced inside or outside the underground laboratory result in a limited contribution to the visibility loss. In practice only the linear part of the estimator was used to derive the fluctuations of the phase.

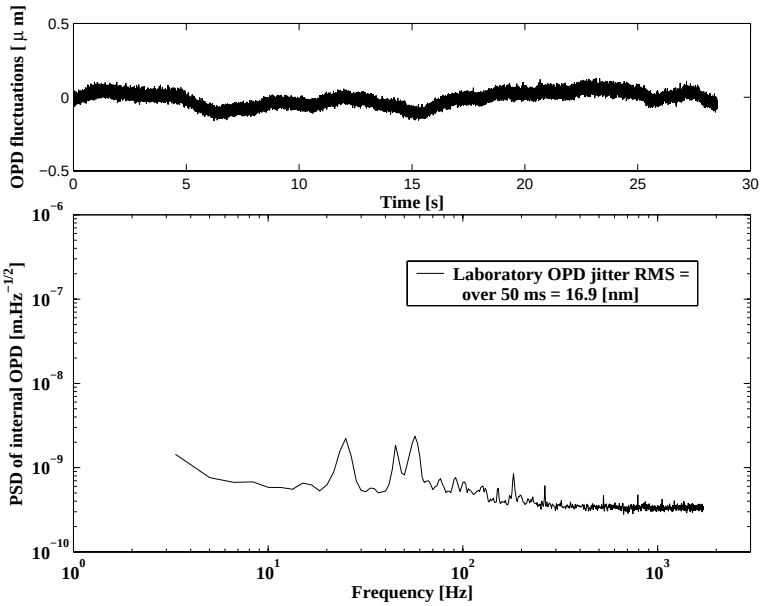

Figure 4. OPD fluctuations measured in the VLTI laboratory and associated PSD proving the stability of the instrument and its environment. Three peaks are observed in the spectrum corresponding to vibrations caused by liquid cooling pumps in UTs enclosures (24 Hz), fans of electronics (45 Hz) and optical tables modes (58 Hz).

Measurements were carried out using artificial star and combining directly the beams in auto-test. They have demonstrated the extreme stability of the VLTI laboratory, where all future instruments will be installed. A very slow drift of the internal laboratory OPD was observed, leading to a global shift of the fringes of about 2.5 microns over 20 min Results are presented in Figure 4, where the PSD is plotted together with the estimated phase fluctuations (converted into OPD variations), leading to OPD jitter of the order of 15 nm rms (averaged over 50ms intervals). The global level of the PSD is below 1 $nm.Hz^{-1/2}$. Three small peaks appear in the spectrum at 24, 45 and 58 Hz. They were identified to be caused respectively by cooling pumps in the UTs enclosures, fans of electronics and optical table mode (results from an accelerometry tests campaign). Considering the global level of the PSD, they do not contain much power and their contribution to the total interferometric visibility loss is negligible.

3. Stability of the Delay Lines tunnel

In order to characterize the internal piston in the delay lines tunnel, corner cubes were installed at the entrance of the light duct. The IR laser beams were combined by VINCI with temporal modulation over 100 μm of OPD. Fringes are sampled with a constant rate of 5 points per fringe, which enables us to derive power spectra up to f ~ 2 Hz. All tests were carried out during the night with atmospheric and thermal conditions in the tunnel absolutely similar to the regular observing conditions with VINCI. Temperature was about 13.5° C in the tunnel and 9° C outside during these measurements, enclosures of the telescopes were open, and thus enabling the air mixing between inside and outside, the external wind speed was around $5m.s^{-1}$ (typical median value).

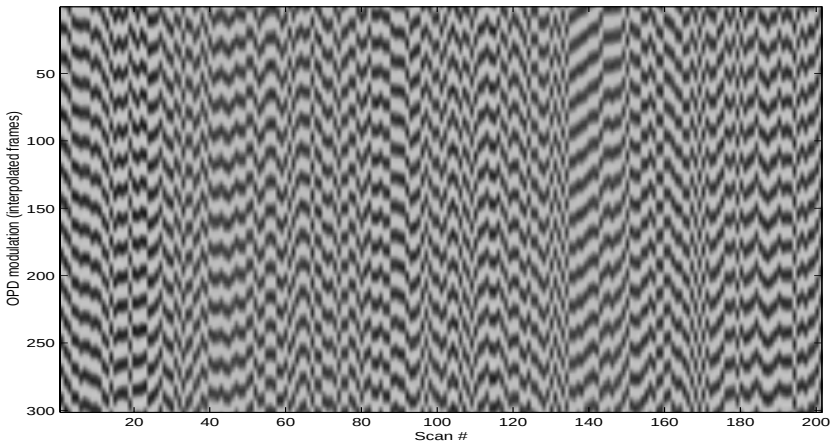

Figure 5. Typical series of modulated laser interferograms recorded in auto-collimation with corner cubes located at the entrance of the light ducts. Scans are vertical, time runs along the abscissa axis (scan frequency was ~4 Hz).

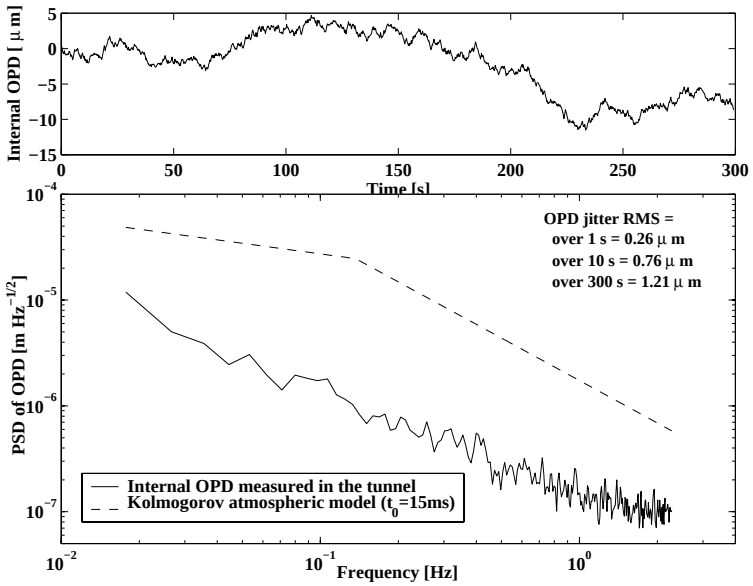

Figure 6. Fluctuations of the internal OPD measured in the delay lines tunnel and associated PSD. The measured OPD was divided by 2 in order to be converted into single path OPD representative of the stellar path. The global level of the spectrum is compared to the best atmospheric conditions experienced at Paranal (dashed line, t_0 around 15 ms). The contribution of the internal OPD fluctuations proves to be always much lower than the atmospheric ones.

Figure 5 illustrates the fluctuations of the internal OPD measured in this auto-collimation configuration. The phase was estimated by tracking intensity maxima from a scan to another. The recording spans over several minutes and allows extracting the low frequency behavior of the internal OPD. The power of the OPD fluctuations shown in Figure 6 is low enough to be neglected in comparison with the external atmospheric fluctuations. A Kolmogorov theoretical model is superimposed to the computed PSD, corresponding to the longer coherence time experienced at Paranal (t_0=15 ms at λ=0.5 μm). The standard deviation of the internal piston over this 20 min sequence is less than 2 microns. Koehler [10] reports similar complementary results obtained on the optical path leading to UT1 and UT3.

Finally, the internal OPD variations in the laboratory and in the tunnel have proven to be much lower than those of the atmosphere. Commissioning tasks are still ongoing in order to further increase the global stability of the VLTI.

3. ATMOSPHERIC DIFFERENTIAL PISTON MEASURED WITH VINCI

1. Data

VINCI is not a fringe tracker but was designed to produce interferometric scans with temporal modulation. Typical fringe frequencies range from 250 to 700 Hz on the brightness and visibility of the target. In order to keep the fringe packet within the ~200 μm range during a batch, a coherencing facility has been implemented. This centering algorithm uses scans partly corrected from photometric variations and filtered at the fringes frequency. It applies a threshold to this signal and computes the centroid of the fringes above the threshold. This basic coherencing capability permits to track the fringes envelop but does not make VINCI a phase tracker. It was nevertheless used for our study and the delay line offsets were integrated in order to characterize the strength and the temporal properties of the OPD.

During the first year of commissioning with VINCI, two different baselines have been used with the siderostats, which are 16m and 66m long. Specific data for the characterization of the piston have been recorded on each baseline. Since the maximum speed of the piezo-mirror limits severely its capacity to deliver short scans, the greatest frequency reached so far was 33 Hz on the 16m baseline (30 μm range scans). This allowed computing power spectra up to 16.5 Hz and up to 3 or 4.5 Hz on the 66m baseline (due to a lower correlated magnitude of the brightest sources available).

In all cases, typical OPD sequences lasted about 15 to 18 minutes, comprising several thousands scans each time. Unfortunately, the instability of the flux injection into the optical fibers over such long periods results sometimes in a loss of the fringes, producing gaps in the series of OPD (oscillation and progressive degradation of the SNRs). This study gathers in total more than 35 batches of 15 min duration each on the short baseline and about 20 batches of 18 min each on the long one.

2. Power spectra and estimation of the coherence time

The evolution of the optical path difference was computed by integrating over the time the DL offsets sent by the instrument for fringe centering. Power spectral densities (PSD) of the OPD were then computed, the coherence time is indeed determined by the constant of proportionality of the $f^{-8/3}$ power law in the intermediate frequency range, since the two-sided PSD of the white light fringe jitter can be written:

$$W(f)\left[\mu m^2 Hz^{-1}\right] = 2.84.10^{-4}\,\lambda_0^2 t_0^{-5/3} f^{-8/3} \quad (1)$$

(All results below correspond to single aperture coherence time expressed in the visible at λ_0=0.5 μm in order to enable the comparison with adaptive optics coherence time which is more commonly used.)
Since the temporal spacing of the offsets sent to the delay line is not strictly regular, interpolation of the signal was made on regular time intervals. The effect is not visible in the temporal series but it guaranties that the Fourier transform is not corrupted by an irregular sampling of the signal. This correction affects only the very high frequency range of the spectra and reduces slightly the flattening observed in this domain, especially for the measurements on the 16m baseline which go up to 16 Hz.

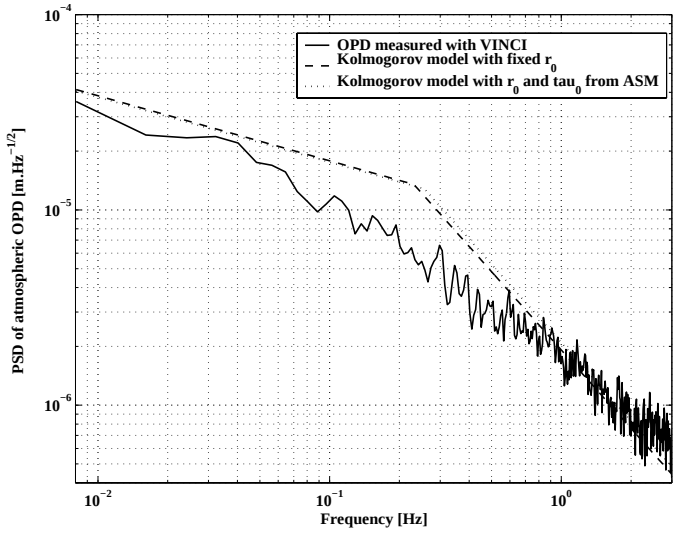

Figure 7. PSD of atmospheric OPD measured on Sirius on the 16m baseline. Only rare spectra are close to the Kolmogorov model (here in good agreement with r_0=15 cm and t_0=2.2 ms estimated by the ASM)

2.1. 16m baseline

On the short baseline, the spectrum shows three different domains corresponding generally at low and intermediate frequencies to the expected behavior of the phase fluctuations and then a progressive flattening above 3-4 Hz. The first two domains are separated by a first knee usually located around 0.5 Hz and corresponding to the cutoff frequency f_1 related either to the baseline length or to a finite outer scale. The flattening at high frequency is partly reduced by the regular time sampling but the level of the fluctuations remains above the predicted Kolmogorov law. The origin of this discrepancy is believed to be due to the inaccuracy of our OPD estimator. This very high frequency domain was finally not taken into account since its large departure from the -8/3 slope would severely bias the estimation of t_0.

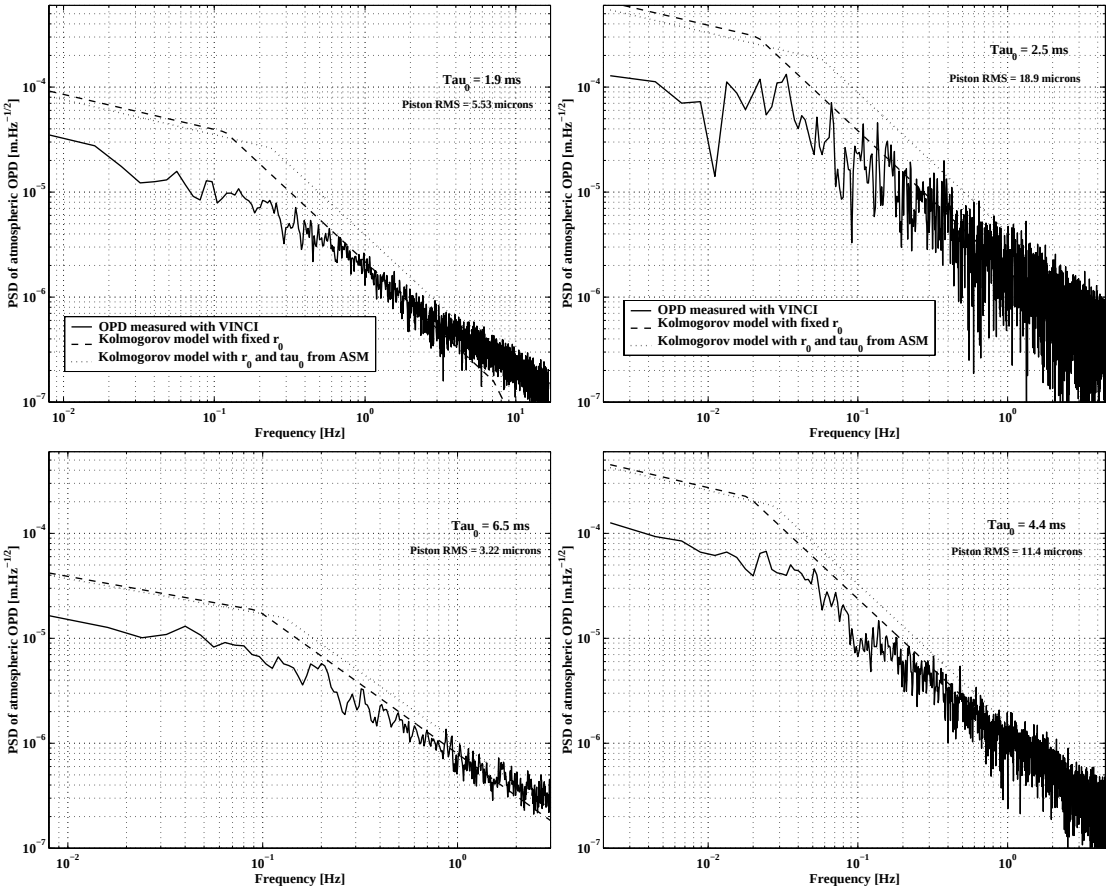

Figure 8. Four typical power spectral densities of the atmospheric OPD fluctuations measured on the 16m (left) and 66m (right) baseline. Low (up) and high (down) level of coherence time are plotted for comparison. Kolmogorov spectra are fitted with frequency break determined with the ASM estimated r_0 and fitted t_0 (dashed line).

The spectral slopes obtained are usually slightly lower than the expected Kolmogorov ones by 10 to 20%. In consequence, estimations of the t0 can be partly biased by this departure. All coherence times derived from this method are larger than those estimated by the combination of the wind speed forecasts above Paranal and r_0 measurements with the ASM (cf section 4). At low frequency, all spectra are below the Kolmogorov power law plotted on Figure 8 (theoretical curves use r_0 and t_0 values determined by the ASM (corrected of the airmass effect). Only a very few batches are fully compatible with the Kolmogorov model (example in figure 7). Possible influence of a finite outer scale is discussed in section 5.

2.2. 66m baseline

On the longest baseline, the central parts of the PSDs show in almost all batches a slope shallower but close to the slope predicted by the theoretical models. Figure 8 presents two typical data sets with high and low coherence time for each baseline for comparison. The total power under the curve is well correlated with the baseline length and values of r_0 and t_0. For each 15 min batch, an $f^{-8/3}$ power law was fitted to the experimental curve in the [0.2-2Hz] domain, where the approximation with the above formula seems to be good in most of the data sets. Results are given in figure 10 for both baselines. These measurements confirm the relatively short coherence time observed in Paranal (typically of the order 3 ms median value). Several batches of various lengths were recorded during 5 nights whereas the data on the 16m baseline span several months. Strong evidences for low frequency saturation suggest the presence of a finite outer scale, see discussion in section 5. Further details on the comparison with ASM data are presented in section 4.

3. Piston strength and velocity

In addition to the coherence time, we derived statistics on the piston speed from our OPD sequences. The velocity was computed from the delay lines offsets applied between each scan and consists then in a very rough estimation. Figure 9 shows a good correlation between the mean piston speed and the estimated coherence time. Information on the velocity of the piston and its statistic can be useful for future fringe trackers since high velocities can cause fringe(s) jumps or fringes lost during the tracking (such velocities depend obviously on the sampling frequency used).

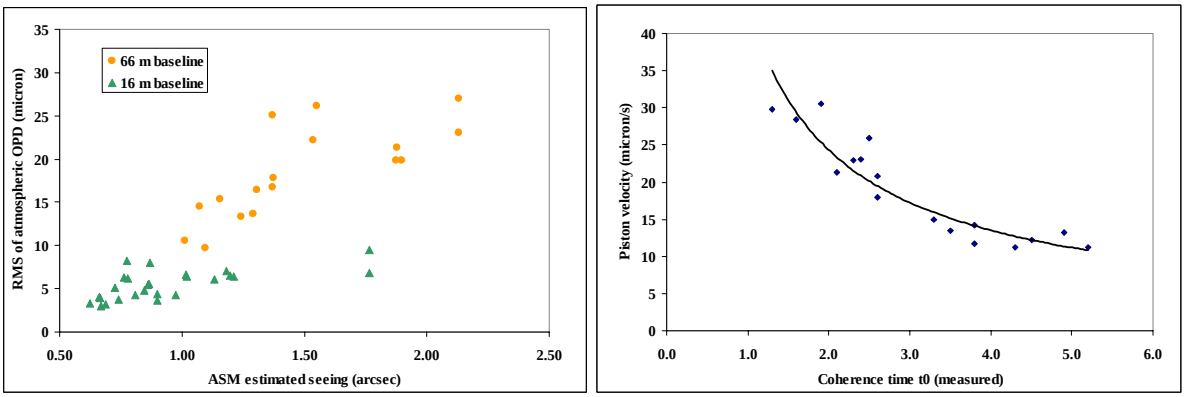

Figure 9 Variation of the OPD fluctuations (left) and OPD velocity (right) with the atmospheric parameters

The variance of the piston can also be derived. It depends both on the baseline length and on the Fried parameter r_0, this latter is linked to the coherence time via the effective wind speed in the turbulent layer and the variance of the piston shows therefore strong correlation with the evolution of t_0. The variation with the B of the variance of the OPD jitter suggests the presence of an outer scale greater than the shortest baseline used for these measurements (see §5).

4. Comparison of the measured coherence time with ASM estimations

4.1. Estimation of the coherence time with the Astronomical Site Monitor

Since the first fringes with VINCI on the siderostats (March 2001), real time estimations of the coherence time are available, thus helping the observers to choose the best scanning frequency in order to limit the influence of the piston speed on the degradation of the visibilities precision. These estimations are partly based on the theoretical formula which links the Fried parameter and the coherence time, and on wind speed forecasts. The velocity of the turbulence is estimated using the model proposed by Sarazin&Tokovinin ([14]) for the Chilean sites: $V_0 \cong \mathrm{Max}\ (V_{ground}, 0.4\ V_{200mb})$. V_{ground} is measured in real time at different levels above the platform and V_{200mb} states for the characteristic of the subtropical jet stream, measured at 200 mb (12km above see level). The 6-hourly forecast of V_{200mb} are interpolated and combined with 10 min averages of V_{ground} in order to derive V_0. The seeing is measured with the DIMM monitor. The accuracy of this method is estimated to be about 20% rms.

4.2. Comparison with our measurements

Comparing our results with ASM estimations shows a nice correlation plotted separately for both baselines on figure 10. The relative evolution of the coherence time given by the ASM is confirmed by our measurements. However, our evaluations of t_0 always lead to larger coherence times, despite the large dispersion of the values which is though to be caused by the low precision of our OPD estimator. They confirmed the relatively low value of the coherence time observed at Paranal with the DIMM monitor, around 3ms median value. Further development of fringe packet centering algorithms should improve our OPD estimation (using wavelet transforms) and thus lead to more accurate results. The proportionality factor of ~1.5 between both estimations could be due to biases in our processing. Further investigation is required before we could conclude on the absolute values of t_0.

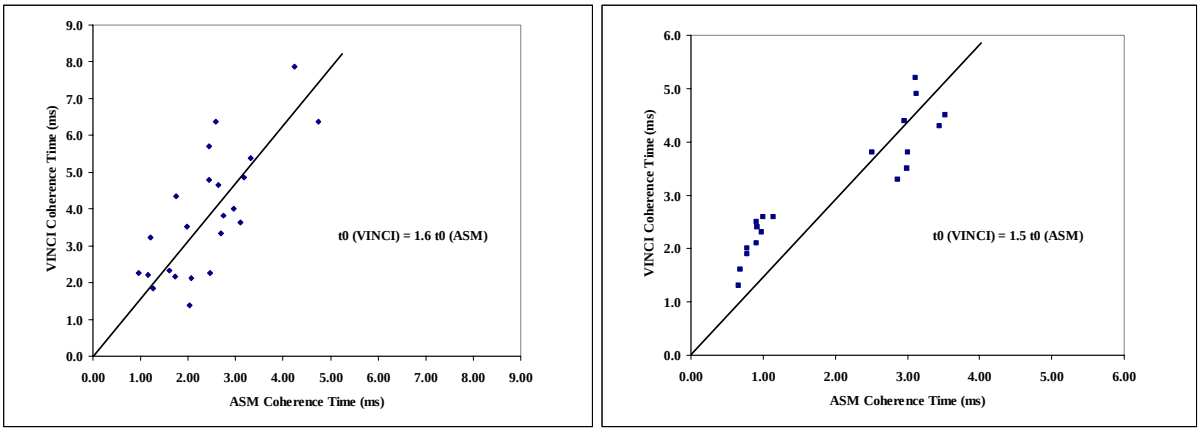

Figure 10 Correlation of the measured coherence time with ASM estimation on the 16m (left) and 66m (right) baselines. The higher dispersion on the short baseline is due to a larger number of observing nights.

5. Constraints on the outer scale length

Most of spectra on the 66 m baseline show saturation below f~0.1 Hz and all spectra on the 16m baseline are below the Kolmogorov expected behavior. This can be linked to an outer scale effect, but considering the limited duration of the batches, it is sometimes difficult to discriminate between saturation of the OPD jitter due to a finite L_0 and a Von Karman or Greenwod-Tarazano model in which the spectrum tends more slowly towards a saturation asymptote. It seems nevertheless possible to extract a minimum value for the outer scale from the cutoff frequency (the possible drift of the zero-OPD due to the imperfection of the DL OPD model was subtracted before computing the PSDs).

In order to estimate a minimum value for the outer scale, the mean effective wind speed was derived from our estimation of the coherence time and from the ASM estimation of the seeing (corrected for the airmass effect). The minimum value of L_0 corresponds to the highest possible cutoff frequency f_0 in the PSD. It appears that our data are consistent with outer scales larger than foreseen, of the order of 120 m instead of the typical 24 m mean value derived by Conan et al 2000. The precision of our estimations is about 10 to 20 % regarding the uncertainty on t_0. Figure 11 shows a spectrum obtained on the 66m baseline with a clear evidence of the presence of a finite outer scale.

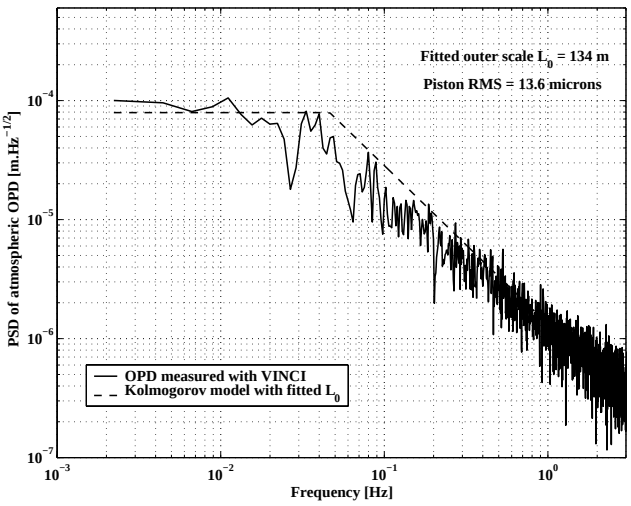

Figure 11 A typical spectrum observed on the 66m long baseline where the saturation due to a finite outer scale is evidenced. Estimations of L_0 are derived from the determination of the wind speed in the turbulent layer using measured t_0 (VINCI) and r_0 (ASM). We obtained values ranging from 80 to 160 m but spread over only 5 nights in August 2002.

4. CONCLUSION

First technical measurements with the commissioning instrument of the VLTI have demonstrated along the first year of operation the satisfying stability of the internal OPD fluctuations. They have been demonstrated to be much lower than the atmospheric piston effect and should not affect the accuracy of the measured stellar visibilities. The level of the spectrum of the long period fluctuations is about a decade below the level of the best atmospheric piston experienced at Paranal.

Atmospheric OPD fluctuations analysis has shown a good correlation between our measurements and the ASM estimations of the coherence time. The spectra computed from our OPD measurements show a small departure from the theoretical Kolmogorov slopes which can probably be partially attributed to the current data processing. Nevertheless, the relatively low values of t_0 observed so far have been confirmed. Median value seems to be around 3-4 ms for 2001. It was also possible to constraint the length of the outer scale and it resulted in a minimum value of L_0 estimated to be around 120m for the 5 nights taken into account on the 66m long baseline, for which we dispose of enough information on the low frequency domain. Further development of intra-scan OPD estimators should help us to improve the quality our spectra and thus to conclude on the absolute values of the coherence time seen by VINCI.

The first fringe tracker of the VLTI, FINITO, will be installed at Paranal in 2003. This will help to overcome the current limitation to the stellar visibility measurements caused by the differential piston effect. A better knowledge of the atmospheric parameters will also benefit from the implementation of this new instrument.

REFERENCES

1. Buscher D. et al., 1995, "Interferometric seeing measurements on Mt. Wilson: power spectra and outer scales", Appl. Opt. **34**, 1081-1096
2. Cassaing F. et al., "An optimized fringe tracker for the VLTI/PRIMA instrument", in Interferometry in Optical Astronomy, P.J. Léna and A. Quirrenbach, eds. Proc. SPIE **4006**, 152-163 (2000)
3. Colavita M., Shao M., Staelin D., Appl. Opt. **26** 4106, 1987
4. Conan J.M., Rousset G., Madec P.-Y., 1995, "Wave-front temporal spectra in high resolution imaging through turbulence", J. Opt. Soc. Am. A/Vol **12**, No. 7
5. Conan R., Ziad, A., Borgnino J., Martin F., Tokovinin A., "Measurements of the wave-front outer scale at Paranal: influence of this parameter in interferometry ", in Interferometry in Optical Astronomy, P.J. Léna and A.Quirrenbach, eds. Proc. SPIE **4006**, 963-973 (2000)
6. Coudé du Foresto V., "Deriving object visibilities from interferograms obtained with a fiber stellar inteferometer", A&A Suppl. S. **121**, 379-392 (1997)
7. P. Kern, F. Malbet, J.-Ph. Berger, P. Haguenauer, K. Rousselet-Perraut, C. Perrier-Bellet, "Increasing the imaging capabilities of the VLTI using integrated optics", These Proceedings, SPIE **4838-76** (2002)
8. Kervella P. et al., "VINCI: The VLT Interferometer Commissioning Instrument", in Interferometry in Optical Astronomy, P.J. Léna and A. Quirrenbach, eds. Proc. SPIE **4006**, 31-42 (2000)
9. Kervella P. et al., "VINCI, the VLTI commissioning instrument: status after one year of operations", in these Proc. **4838-152** (2002)
10. Koehler B., Lévêque S., Gitton Ph., "A decade of VLTI technical development", in these Proc. **4838-151** (2002)
11. Linfield R., Colavita M. and Lane B., 2001, "Atmospheric turbulence measurements with the Palomar Testbed Interferometer"
12. Nightingale N.S. & Buscher, D.F., 1991, "Interferometric seeing measurements at the La Palma Observatory", MNRAS **251**, 155
13. Roddier F., "The effects of atmospheric turbulence in optical astronomy", in Progress in Optics, E. Wolf ed., Vol. XIX, 281-376, 1981
14. Sarazin M., Tokovinin A., "The statistics of isoplanetic angle optics time constant derived from DIMM data", Conf. Proc. "Beyond Conventional Adaptive Optics", Venice 2001